

# Nonlinear Optics (WiSe 2017/18)

## Lecture 25: January 25, 2018

### Chapter 13: Strong-field physics in solids

#### 13.3 Semiconductor Bloch equations

(13.4 Carrier-wave Rabi flopping)

(13.5 THG in disguise of SHG)

} in Lecture 19 already

#### 13.6 High-harmonic generation from solids

13.6.1 *Ab-initio* simulations based on TDDFT

#### 13.7 High-order sideband generation

#### 13.8 Dynamical Franz-Keldysh effect

(13.9 Other strong-field phenomena in solids)

# Semiconductor Bloch equations

$$\begin{aligned} & \left( \frac{\partial}{\partial t} + i\hbar^{-1} \left[ \hat{E}_c(\vec{k}) - \hat{E}_v(\vec{k}) \right] \right) p_{vc}(\vec{k}) + \left( \frac{\partial}{\partial t} p_{vc}(\vec{k}) \right)_{\text{scat}} \\ & = i\hat{\Omega}_R(\vec{r}, \vec{k}, t) \left[ f_v(\vec{k}) - f_c(\vec{k}) \right] + e\hbar^{-1} E(\vec{r}, t) \nabla_{\vec{k}} p_{vc}(\vec{k}), \end{aligned} \quad (13.36)$$

**interband**

**intraband**

and

$$\frac{\partial}{\partial t} f_c(\vec{k}) + \left( \frac{\partial}{\partial t} f_c(\vec{k}) \right)_{\text{scat}} = -2\text{Im} \left( \hat{\Omega}_R(\vec{r}, \vec{k}, t) p_{vc}^*(\vec{k}) \right) + e\hbar^{-1} E(\vec{r}, t) \nabla_{\vec{k}} f_c(\vec{k}),$$

**interband**

**intraband**

$$P(\vec{r}, t) = \sum_{\vec{k}} d_{cv}(\vec{k}) \left( p_{vc}(\vec{k}) + \text{c.c.} \right) + P_b(\vec{r}, t), \quad (13.33)$$

$$J(\vec{r}, t) = e \sum_{\vec{k}} \left( v_{cg}(\vec{k}) f_c(\vec{k}) + v_{vg}(\vec{k}) f_v(\vec{k}) \right), \quad (13.38)$$

$$I_{\text{rad}}(\omega) \propto |\omega^2 P(\omega) + i\omega J(\omega)|^2 \quad (13.39)$$

**interband** and **intraband** dynamics are **coupled**

The dependence of the internal structure of a particle on the dynamical parameter can give rise to anomalous transport properties — in particular, the Berry-phase effect<sup>174</sup>. The Berry phase can be characterized by the Berry curvature,  $\Omega$ , which behaves like an effective magnetic field in momentum space. In the context of Bloch electrons — that is, electrons that occupy a Bloch band of a crystalline solid —  $\Omega$  originates from the dependence of the periodic part of the Bloch function,  $u_{n,\mathbf{k}}$ , on the wave vector  $\mathbf{k}$ . Consider a wave packet of a Bloch electron moving adiabatically in a non-degenerate energy band with band index  $n$ . In many situations, the wave packet has a real-space extension that is much larger than the lattice constant but much smaller than the length scale of the external perturbation; thus, the wave vector and the position of the wave packet can be considered simultaneously. The electron wave packet can then be described by the semiclassical transport equations of motion<sup>14,16</sup>:

$$\dot{\mathbf{r}} = \frac{1}{\hbar} \frac{\partial E_{n,\mathbf{k}}}{\partial \mathbf{k}} - \dot{\mathbf{k}} \times \Omega_{n,\mathbf{k}} \quad \hbar \dot{\mathbf{k}} = -e\mathbf{E} - e\dot{\mathbf{r}} \times \mathbf{B}$$

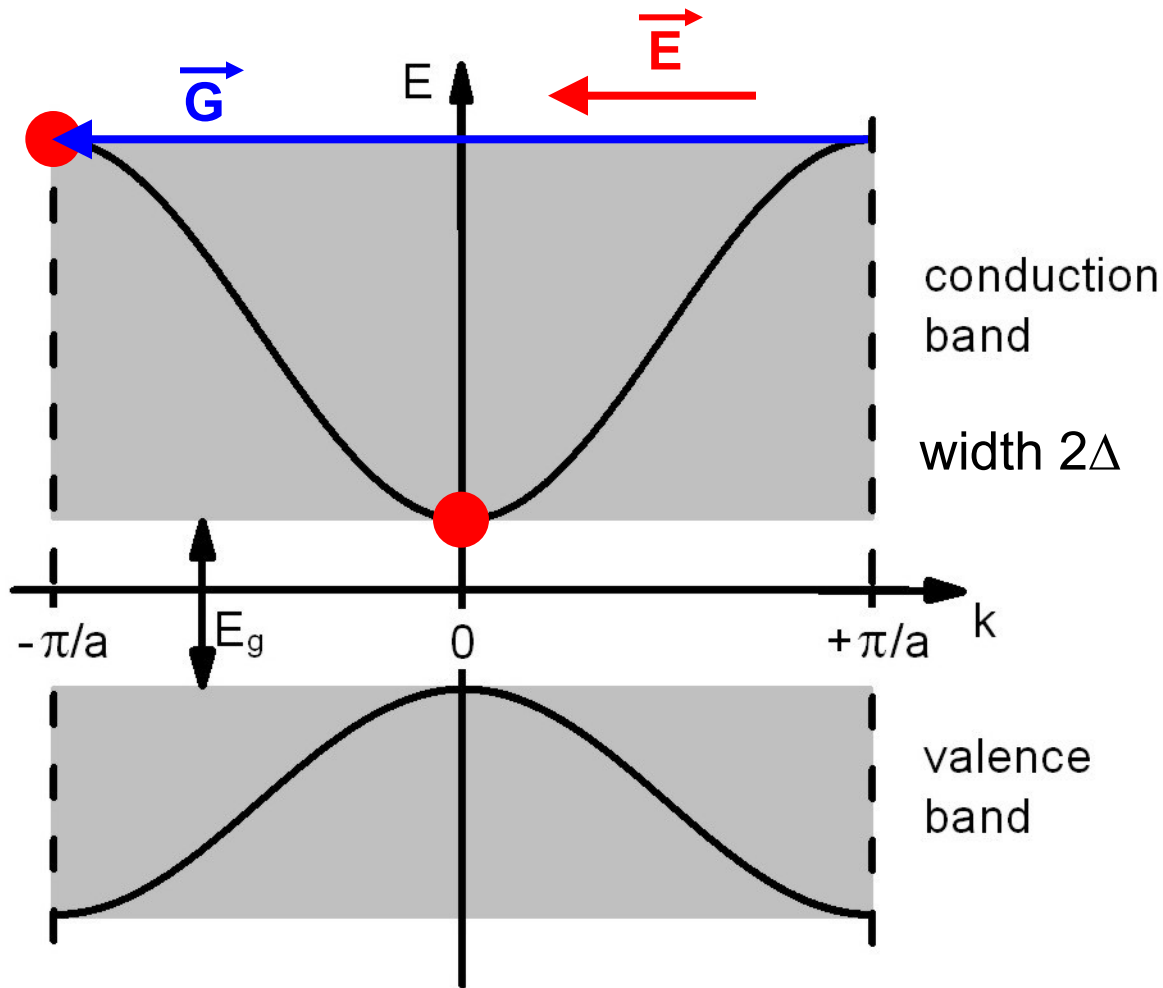
where  $E_{n,\mathbf{k}}$  and  $\Omega_{n,\mathbf{k}}$  are the energy dispersion and Berry curvature of the  $n$ th band,  $\mathbf{k}$  and  $\mathbf{r}$  are the crystal momentum and position of the electron wave packet, and  $\mathbf{E}$  and  $\mathbf{B}$  are the external electric and magnetic field, respectively. The dot represents the first derivative with respect to time. The term  $\dot{\mathbf{k}} \times \Omega_{n,\mathbf{k}}$  gives rise to an anomalous velocity perpendicular to  $\mathbf{E}$  (that is, the Hall effect).

J. R. Schaibley *et al.*, Nature Reviews Materials **1**, 16055 (2016)

D. Xiao, M.-C. Chang, and Q. Niu, Rev. Mod. Phys. **82**, 1959 (2010)

# 13.6 HHG from solids

## Bloch oscillations in bulk solids

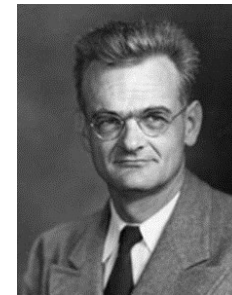


acceleration theorem

$$\vec{F} = \hbar \dot{\vec{k}} = e\vec{E}$$



Felix Bloch,  
Z. Phys. **52**,  
555 (1929)

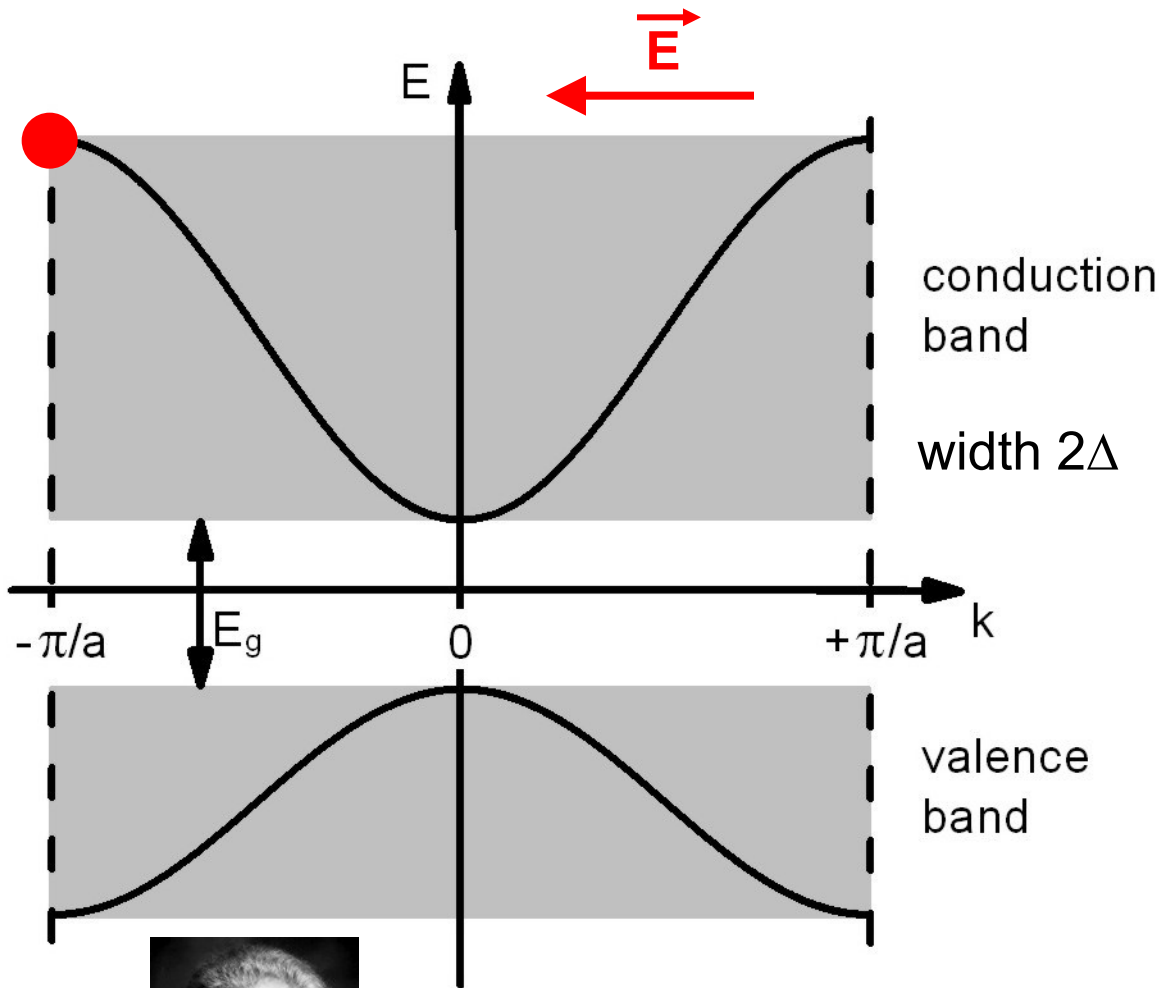


Clarence Zener,  
Proc. R. Soc.  
London A **145**,  
523 (1934)



Gregory H. Wannier,  
Phys. Rev. **117**,  
432 (1960)

# Bloch oscillations in bulk solids



Bloch energy

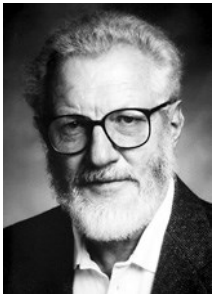
$$\hbar\Omega_B = aeE$$

Bloch period

$$T_B = \frac{h}{aeE}$$

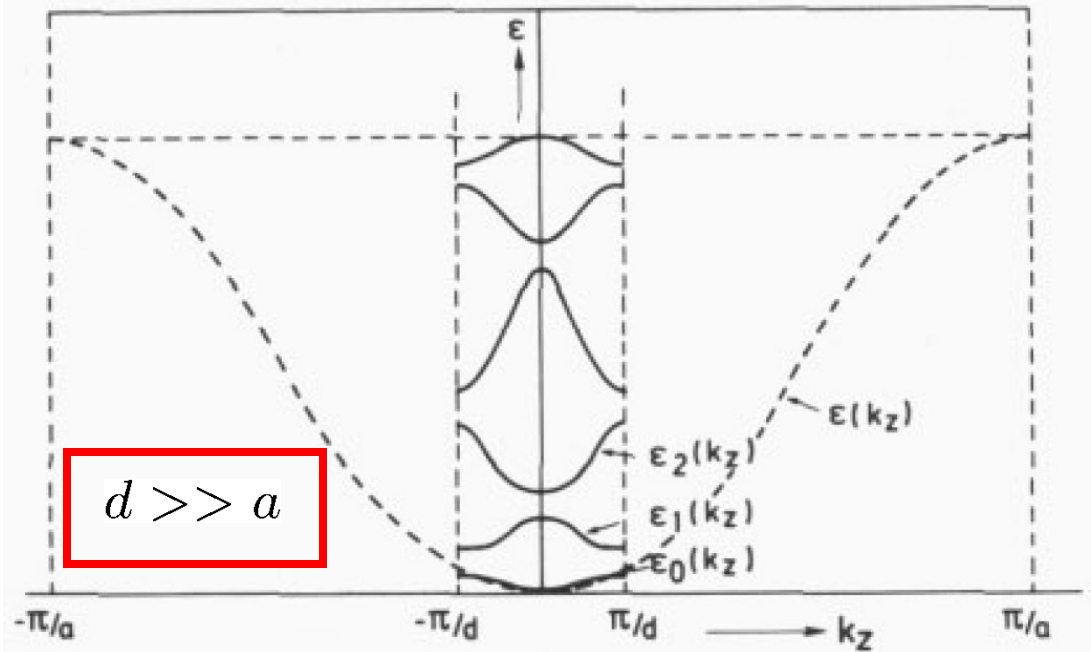
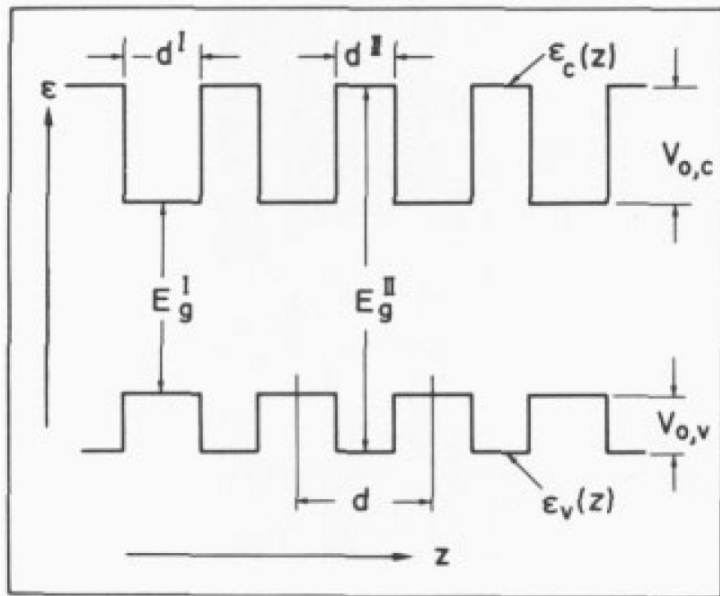
real-space oscillation  
diameter

$$L_B = \frac{2\Delta}{eE}$$



Herbert Kroemer's Nobel Prize autobiography (2000):  
"... it became obvious that the huge fields required for  
Bloch oscillations in a **bulk** semiconductor could never be reached."

# Bloch oscillations in semiconductor superlattices



from G. H. Döhler, *Physica Scripta* **24**, 430 (1981)

Bloch energy  $\hbar\Omega_B = deE$

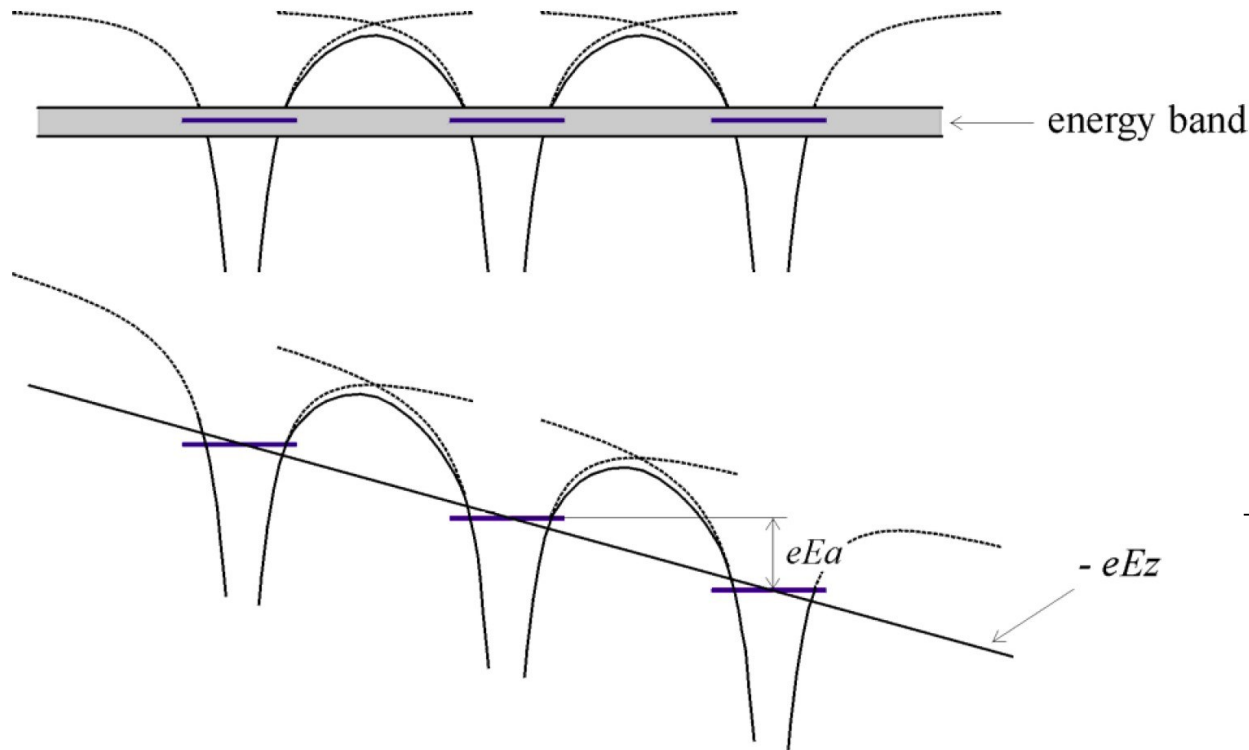
Bloch period  $T_B = \frac{h}{deE}$



L. Esaki *et al.*, *IBM J. Res. Dev.* **14**, 61 (1970):

"If the electron scattering time is sufficiently long, electrons will undergo rf oscillation due to the reflection at the minizone boundaries, the so-called "Bloch oscillation." "

# Wannier-Stark ladders in solids



Wannier-Stark ladder

$$E_m = E_{\text{ref}} + m a e \tilde{E}_0$$
$$m = 0, \pm 1, \pm 2, \dots$$

electron wave packet is **superposition of Wannier-Stark states**,  
**quantum beating** between these states are **Bloch oscillations**

G. H. Wannier, "Wave Functions and Effective Hamiltonian for Bloch electrons in an Electric Field", Phys. Rev. **117**, 432 (1960)

# Equivalence of Bloch-oscillation and Wannier-Stark pictures

Hamiltonian of the system

$$\left[ \frac{\left( -i\hbar\nabla_{\mathbf{r}} - \frac{e}{c}\mathbf{A}(\mathbf{r}, t) \right)^2}{2m_0} + e\varphi(\mathbf{r}, t) + V^{\text{lat}}(\mathbf{r}) \right] \phi_n(\mathbf{r}) = \epsilon_n \phi_n(\mathbf{r})$$

vector-potential gauge:  $\mathbf{A}(\mathbf{r}, t) = -c \int_{t_0}^t \mathbf{E}(t') dt' , \quad \varphi(\mathbf{r}, t) = 0$

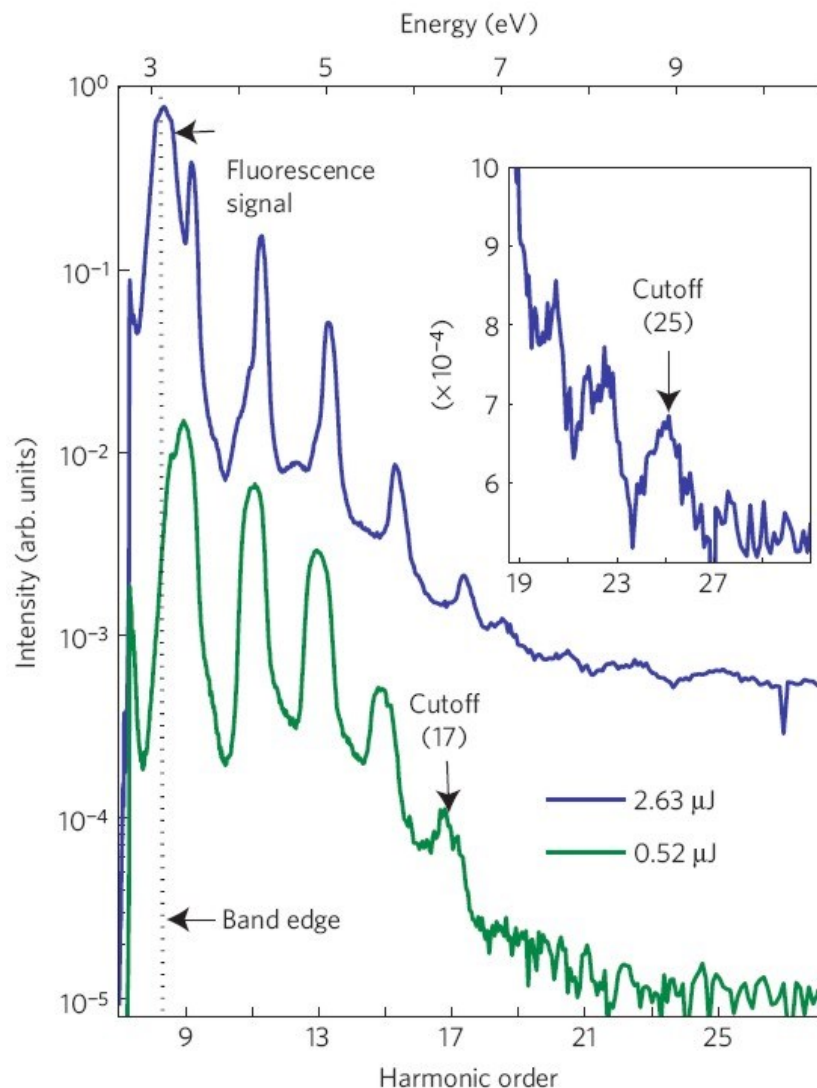
**Bloch-oscillation picture**

scalar-potential gauge:  $\mathbf{A}(\mathbf{r}, t) = 0 , \quad \varphi(\mathbf{r}, t) = -\mathbf{E}(t) \cdot \mathbf{r}$

**Wannier-Stark picture**

total equivalence of the Bloch-oscillation and Wannier-Stark pictures, i.e., the often so-called “semiclassical Bloch picture” is on the contrary a **rigorous quantum-mechanical result** (Fausto Rossi, 1997)

# mid-IR-driven HHG from bulk ZnO



S. Ghimire *et al.*,  
Nature Physics **7**, 138 (2011);  
PRL **107**, 167407 (2011)  
**PRA 107, 167407 (2012)**

500- $\mu\text{m}$ -thin ZnO crystal

9-cycle-long MIR pulses  
( $\sim 100$ -fs  $3.25\text{-}\mu\text{m}$   $0.38\text{-eV}$   
pulses with up to  $2.63\text{ }\mu\text{J}$   
energy, yielding a focused  
field strength of  $6\text{ V/nm}$ )

Bloch HHG up to 25th  
order extending to  $>9.5\text{ eV}$

J. P. Marangos, Nature Physics **7**, 97  
(2011): "An important question not yet  
addressed is whether the harmonic  
emission retains a subfemtosecond  
character; that is, is it confined only to  
certain moments within the optical cycle?  
The observed bandwidth of the emission  
( $\sim 9\text{ eV}$ ) is sufficient to support  
subfemtosecond pulses."

# Bloch oscillation of an electron

“acceleration theorem“:  $\hbar \frac{d}{dt} k = eE$

time-dependent field:  $a \frac{d}{dt} k(t) = -\Omega_B(t)$

instantaneous Bloch energy:  $\hbar \Omega_B(t) = aeE(t)$

solution:  $k(t) = k_0 + eA(t) / \hbar$  with  $A(t) = -\int_{-\infty}^t dt' E(t')$

$k$ -space dynamics directly reproduces  $A(t)$ , however, folded into the first Brillouin zone via Bragg reflections at the Brillouin zone boundaries

# HHG from Bloch oscillating electron wave packets

tight-binding band structure:  $\hbar \omega_e(k) = \frac{\hbar^2}{m_e a^2} [1 - \cos(ka)]$

Boltzmann equation (scattering ignored):  $\frac{\partial}{\partial t} f(k, t) = -\frac{e}{\hbar} E(t) \frac{\partial}{\partial k} f(k, t)$

group velocity:  $v_g(k) = \frac{d}{dk} \omega_e(k)$

resulting current:  $j(t) \propto e \int_{\text{BZ}} dk v_g(k) f(k, t)$

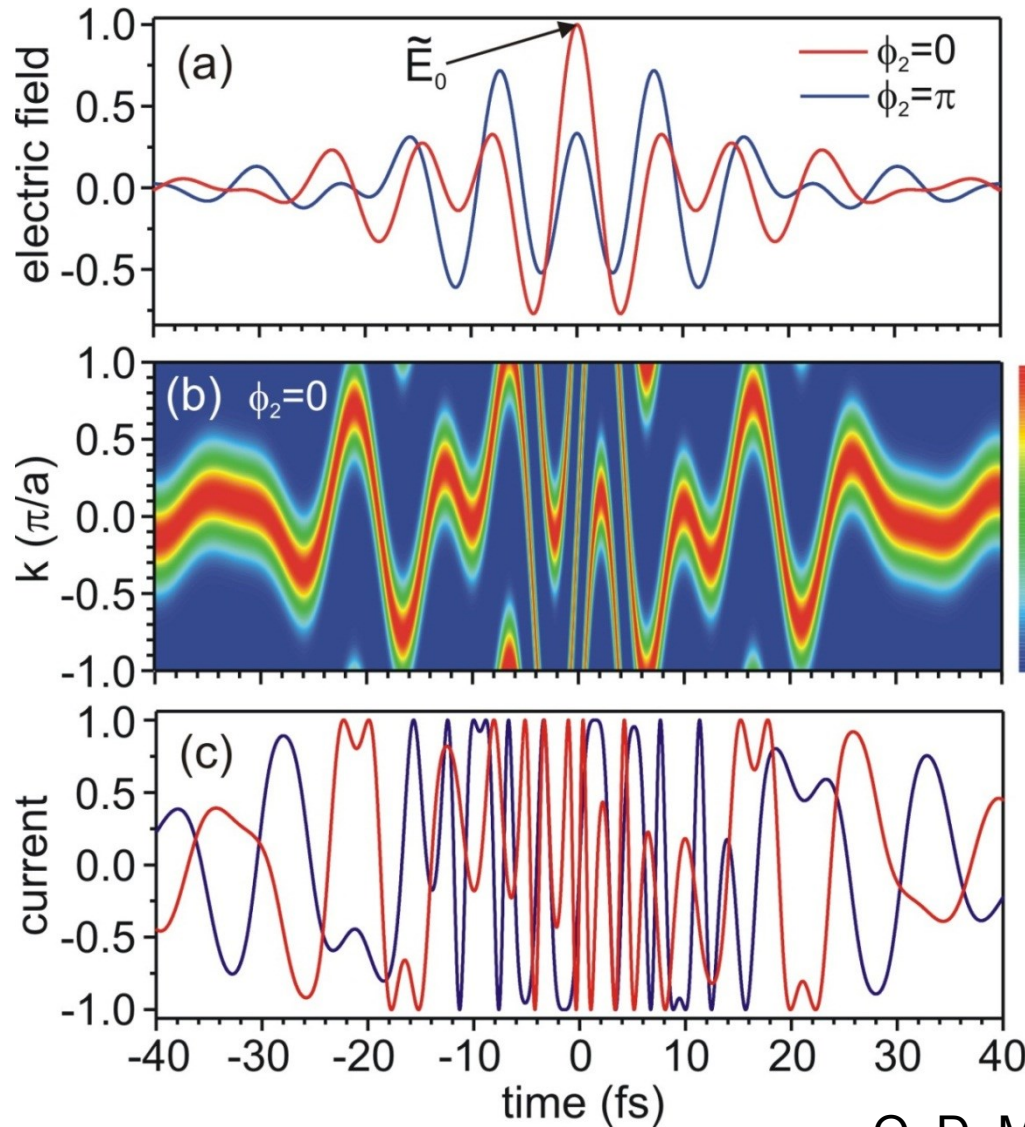
source term  $\partial j(t) / \partial t \rightarrow$  Bloch-HHG spectrum  $I_{\text{rad}}(\omega) \propto |\omega j(\omega)|^2$

M. W. Feise *et al.*, Appl. Phys. Lett. **75**, 3536 (1999)

M. Wegener, *Extreme Nonlinear Optics* (Springer, Berlin, 2005)

O. D. Mücke, PRB **84**, 081202(R) (2011)

# Bloch oscillating electron wave packet



field 1: (17 fs, 2.3  $\mu\text{m}$ ),  
field 2: ( $r_2 = 0.5$ , 25 fs, 3.6  $\mu\text{m}$ )  
 $\tilde{E}_0 = 6.2$  V/nm  
(potential drop of 3V over a)

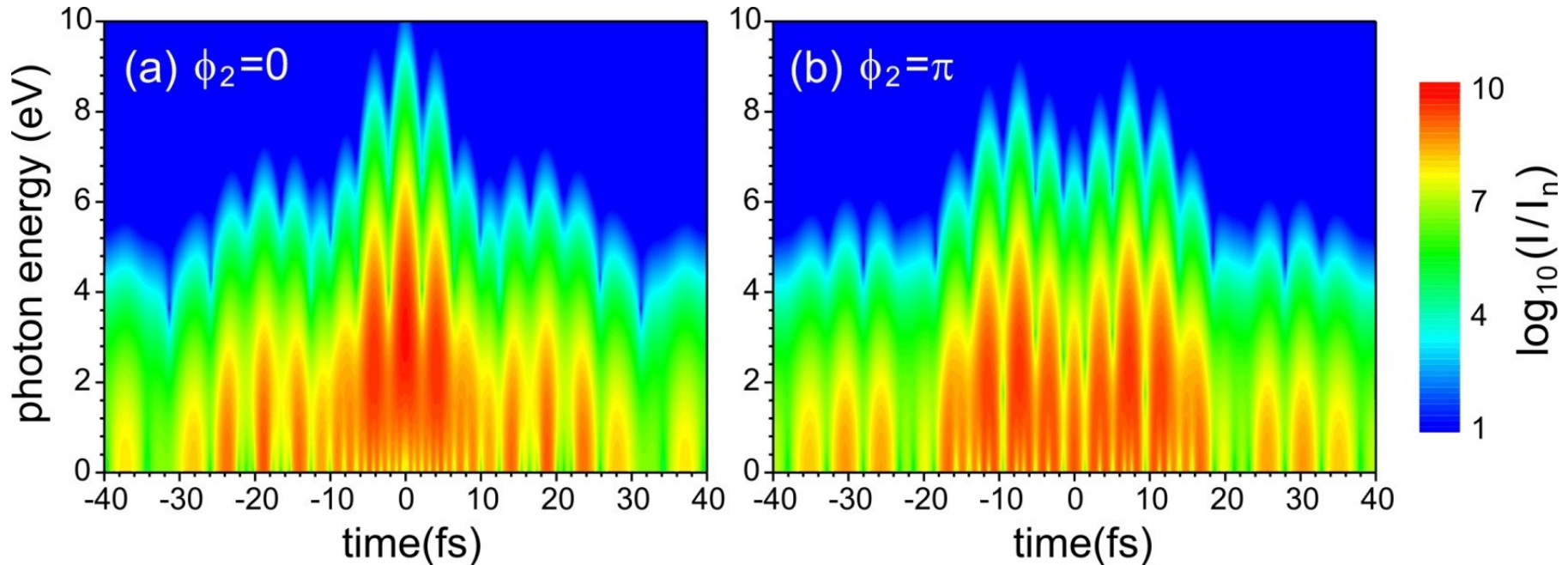
$$k(t) = k_0 + eA(t) / \hbar$$

near  $t=0$ fs, current changes  
from -1 to +1 within 640 as

- O. D. Mücke, PRB **84**, 081202(R) (2011)  
S. Ghimire *et al.*, Nature Physics **7**, 138 (2011)  
O. D. Mücke *et al.*, Opt. Lett. **27**, 2127 (2002)

# Time-frequency analysis using Gabor transform

$$H(\omega, t) = \left| FT_{t'} \left\{ \frac{\partial j(t')}{\partial t} e^{-(t-t')^2/T_G^2} \right\} \right|^2 \quad T_G = 0.7 \text{ fs}$$

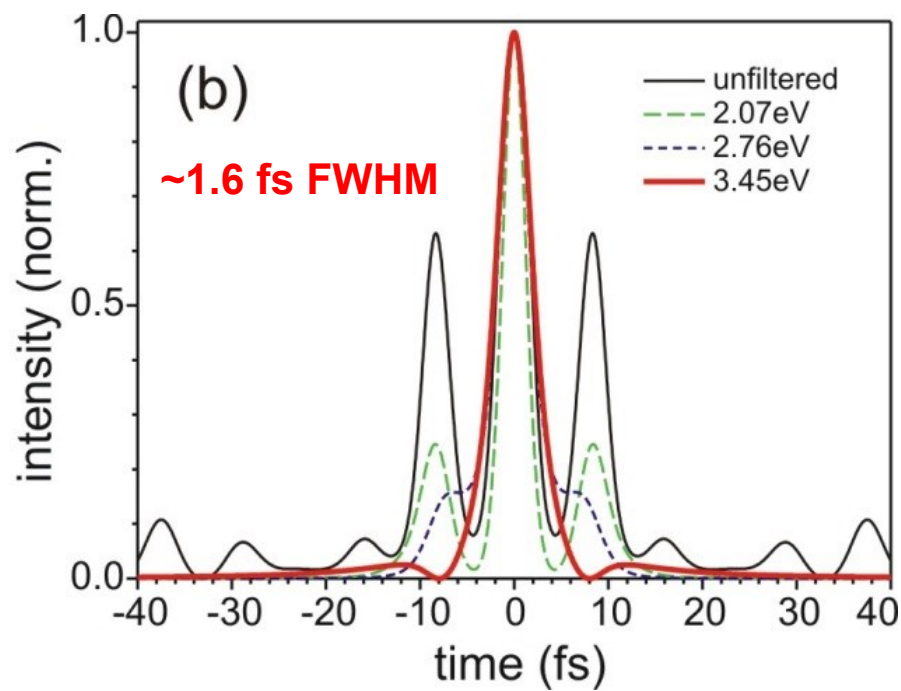
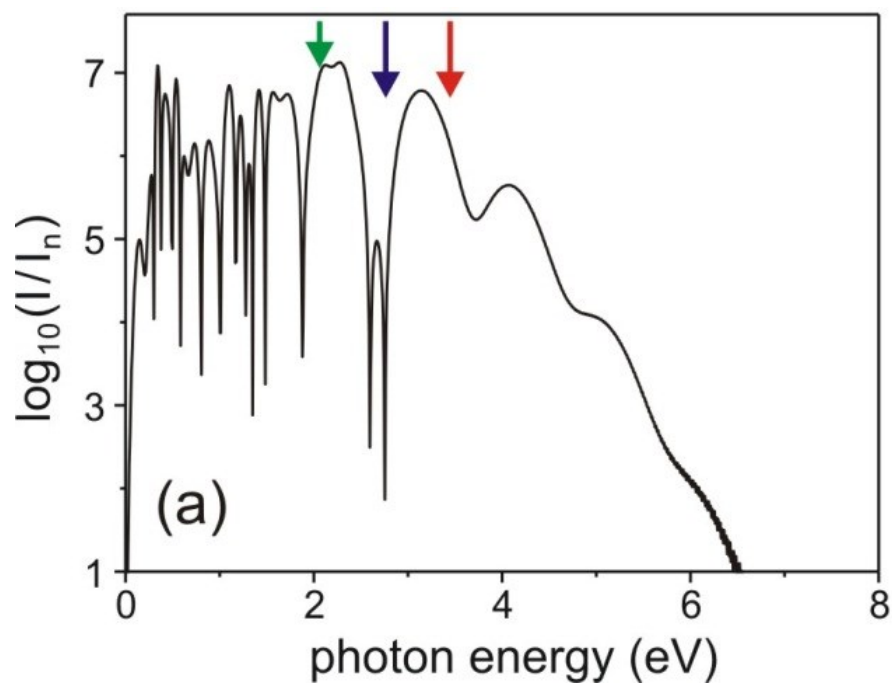


lower harmonic orders: emitted at several instants during one optical cycle

highest harmonic orders: emitted only during extrema of electric field

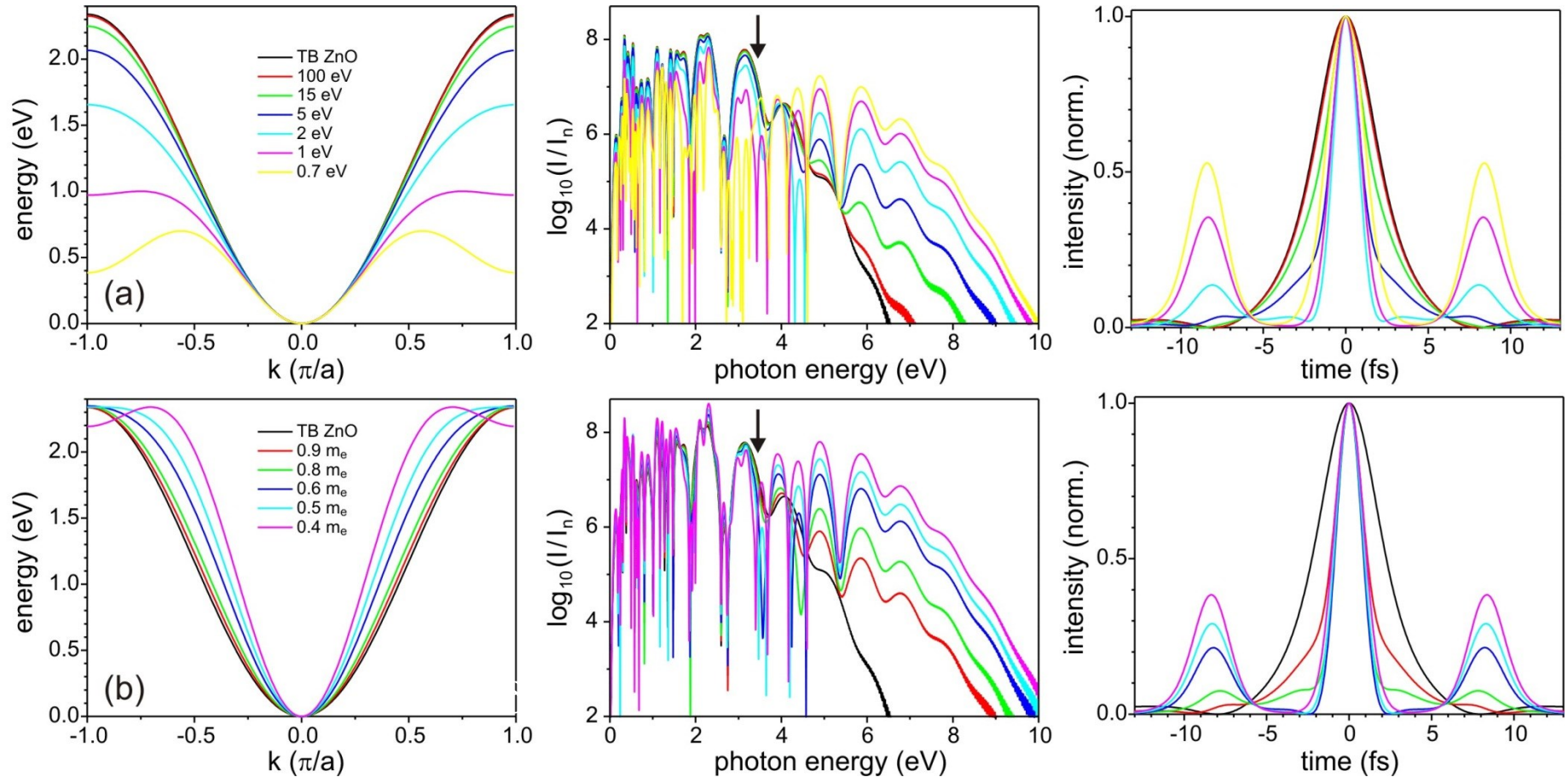
Important: It is obviously NOT feasible to compress the total ~9 eV bandwidth to an isolated attosecond pulse because of the complicated chirp

# Cutoff filtering of Bloch-HHG



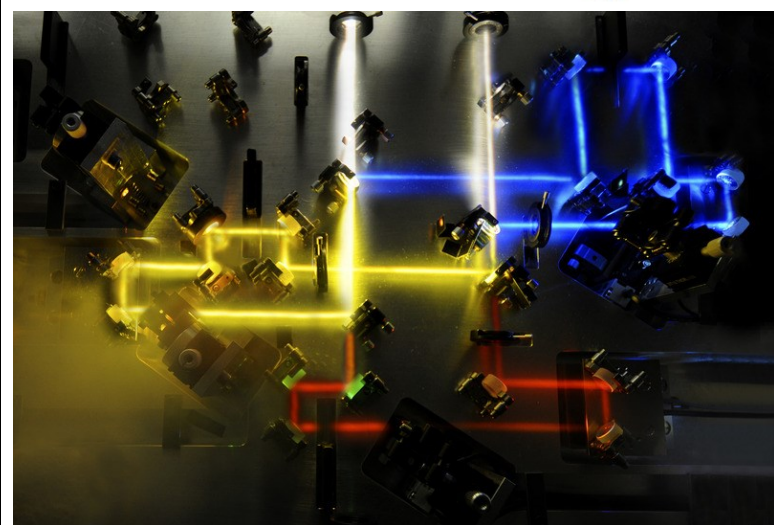
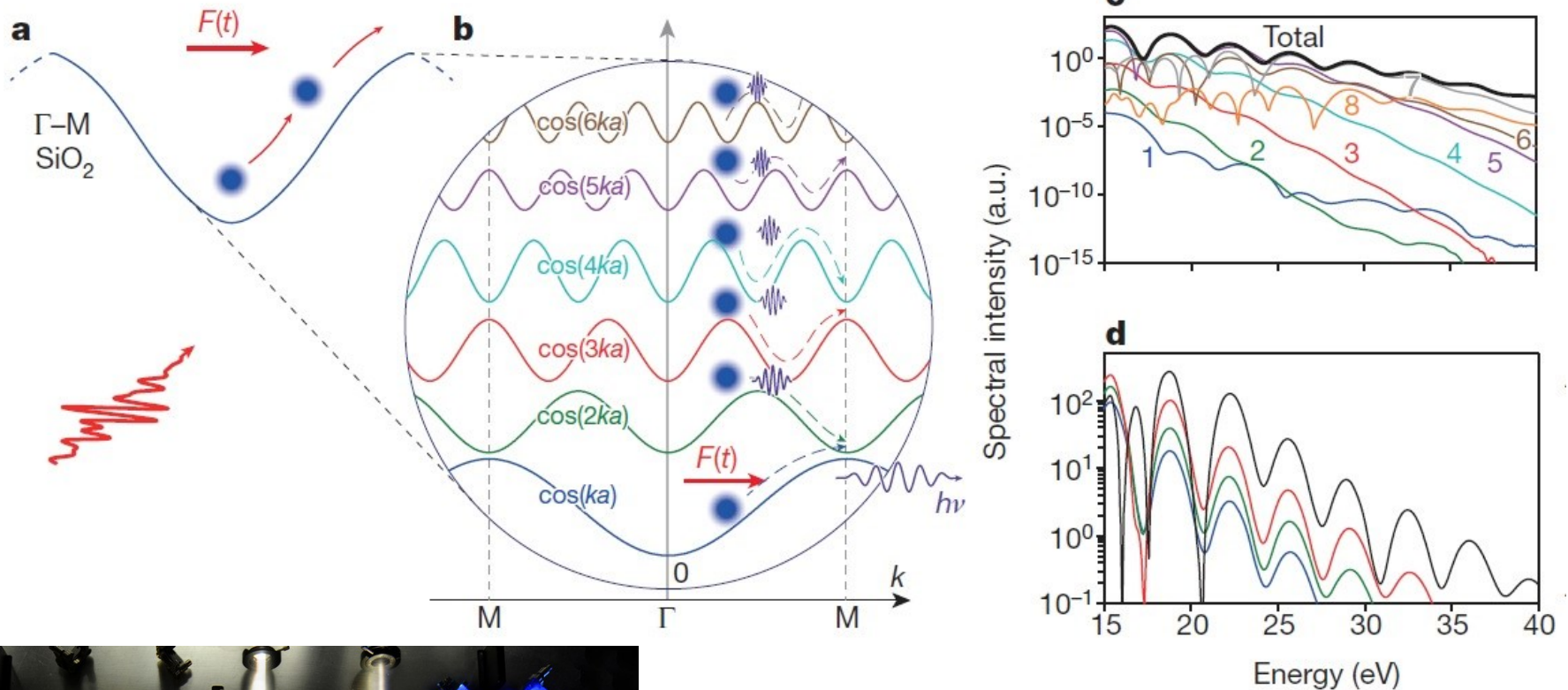
isolated Bloch-HHG pulse of ~1.6-fs FWHM duration

# Influence of band structure



broadness of HHG emission is mainly determined by the maximum steepness of the band dispersion  $\omega_e(k)$  since for a steeper dispersion the intraband acceleration leads to a faster variation of the electron energy via  $k(t)$

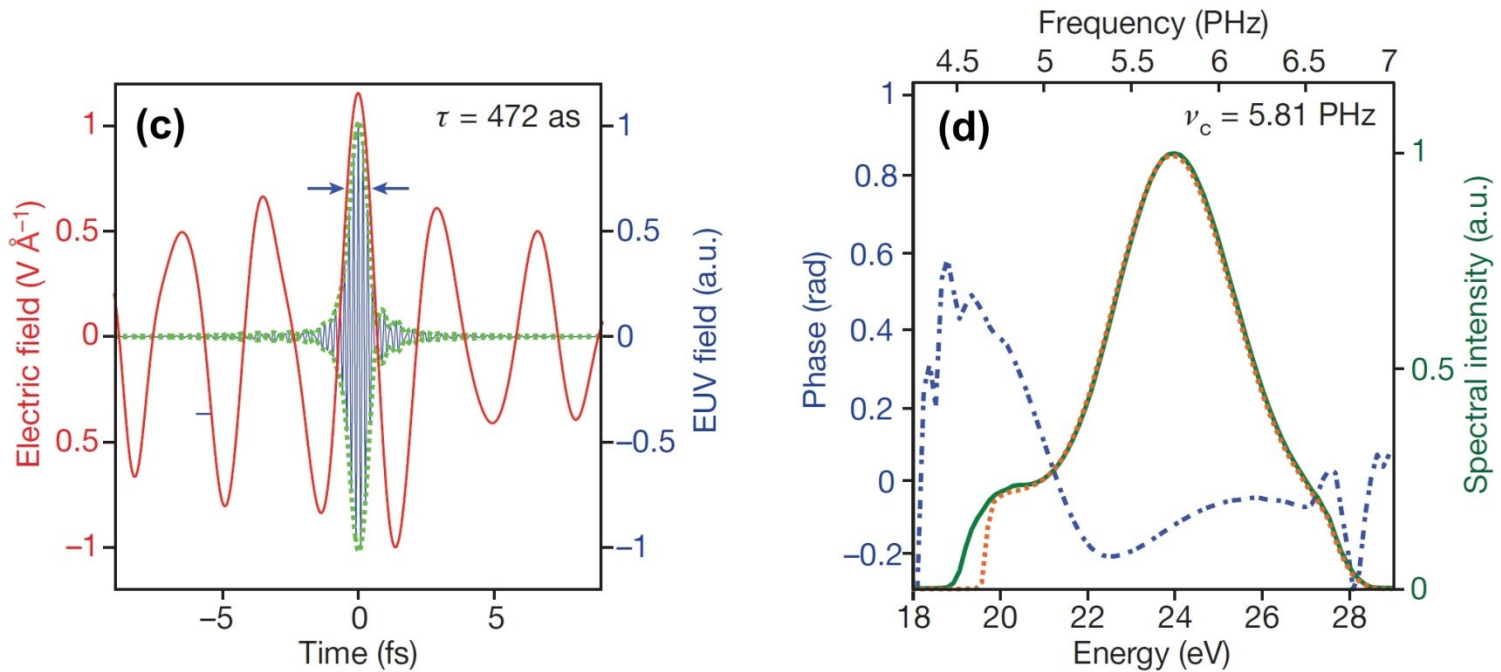
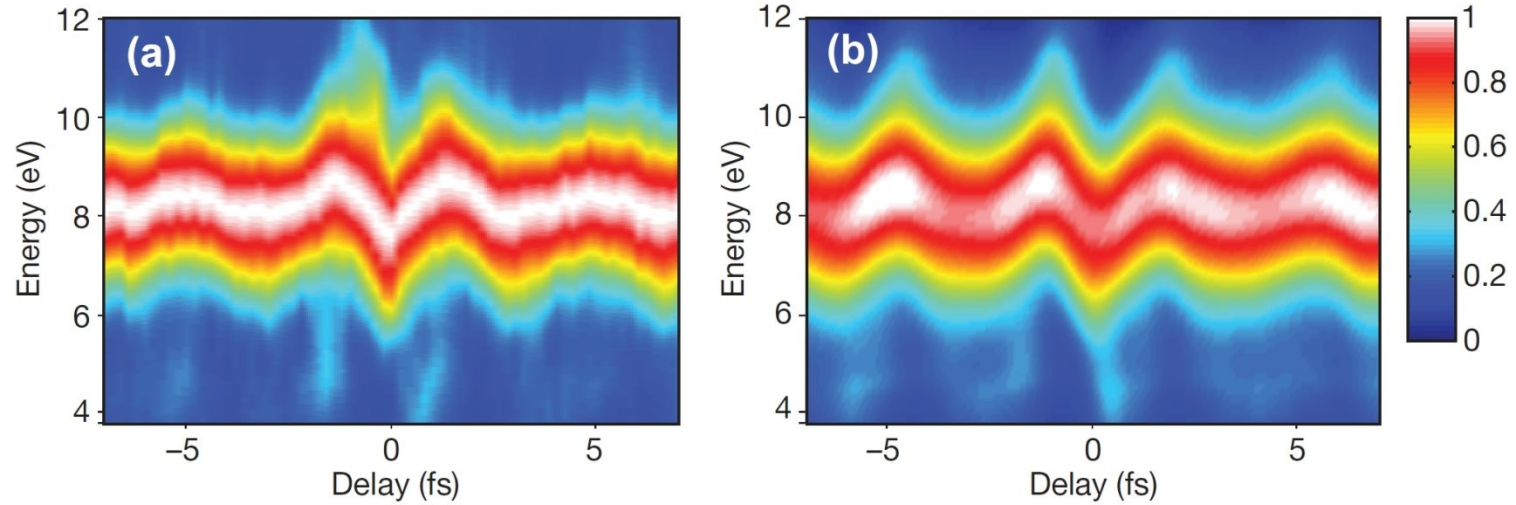
# Waveform-driven HHG from solids: intraband dynamics



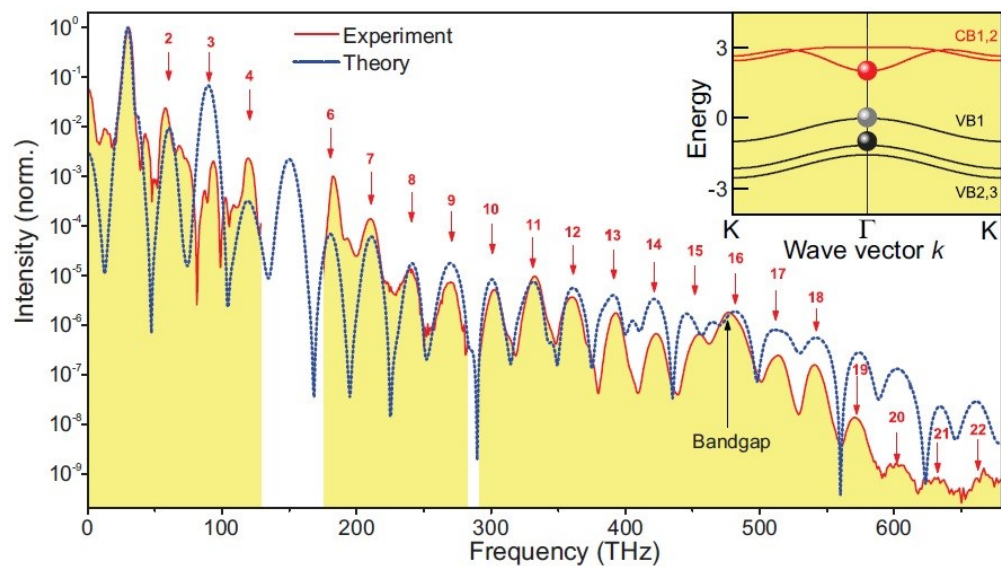
T. T. Luu *et al.*, Nature **521**, 498 (2015)  
M. Garg *et al.*, Nature **538**, 359 (2016)

**intraband** dynamics (Bloch oscillations)

# Waveform-driven HHG from solids: intraband dynamics

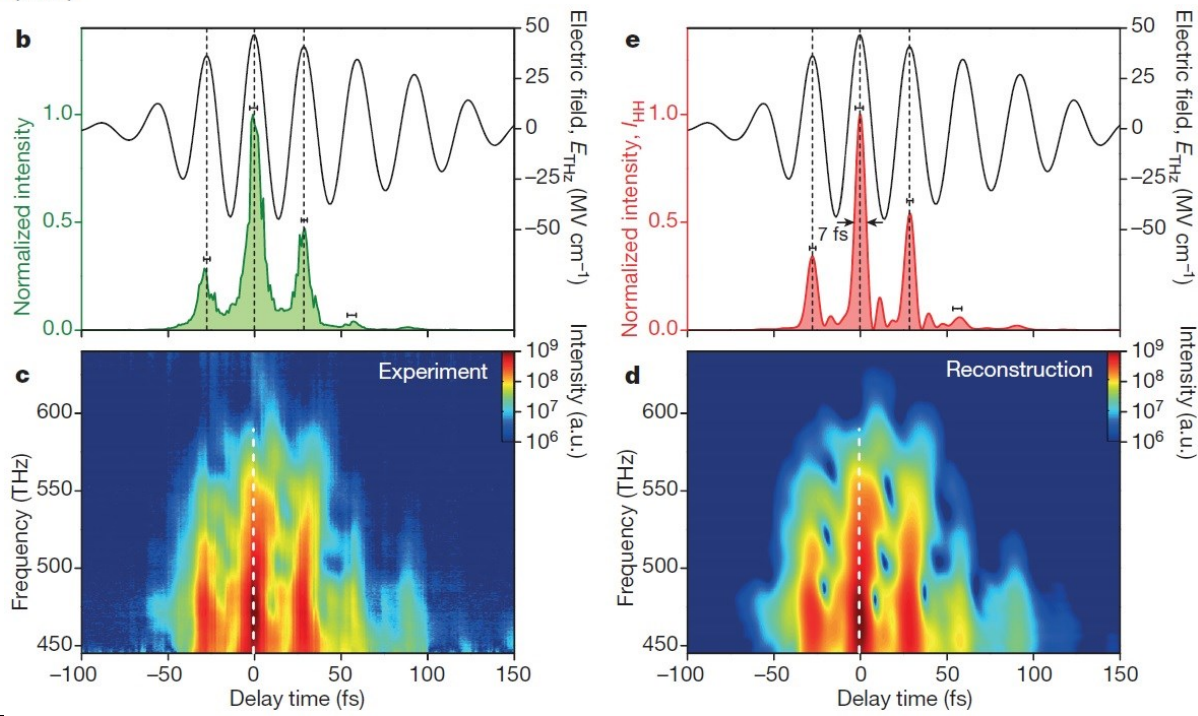


# THz-driven HHG from solids: coupled intra-/interband dynamics



O. Schubert *et al.*,  
Nature Phot. **8**, 119 (2014)

M. Hohenleutner *et al.*,  
Nature **523**, 572 (2015)



## 13.6.1 *Ab-initio* simulations based on time-dependent density-functional theory (TDDFT)

no *a priori* model assumptions, no strong approximations

full electronic structure (valence and conduction bands), real crystal structure

N. Tancogne-Dejean *et al.*, Phys. Rev. Lett **118**, 087403 (2017)

$$\text{HHG}(\omega) \propto \left| \text{FT} \left\{ \int_{\Omega} d^3\mathbf{r} n(\mathbf{r}, t) \nabla v_0(\mathbf{r}) \right\} + N_e \mathbf{E}(\omega) \right|^2. \quad (13.56)$$

like HHG spectrum. The more interesting and relevant term for HHG is the first one in Eq. (13.56). It shows that higher harmonics are generated by two competing terms, the spatial variation of the total electronic density ( $n(\mathbf{r}, t)$ ) and the gradient of the electron-nuclei potential ( $\nabla v_0(\mathbf{r})$ ), the latter being time independent, as ionic motion is neglected here. In gases, the gradient of the electron-nuclei potential is important, but the electronic density is low. In the case of solids, the electronic density is higher, but the potential is rather homogeneous, resulting in a smaller gradient of the potential than in the atomic case. In fact, in the limit of a homogeneous electron gas, the gradient becomes zero, and no harmonics are generated, irrespective of the value of the electronic density. In this case the bands are parabolic, thus we recover the known result that parabolic bands do not yield non-perturbative harmonics [69].

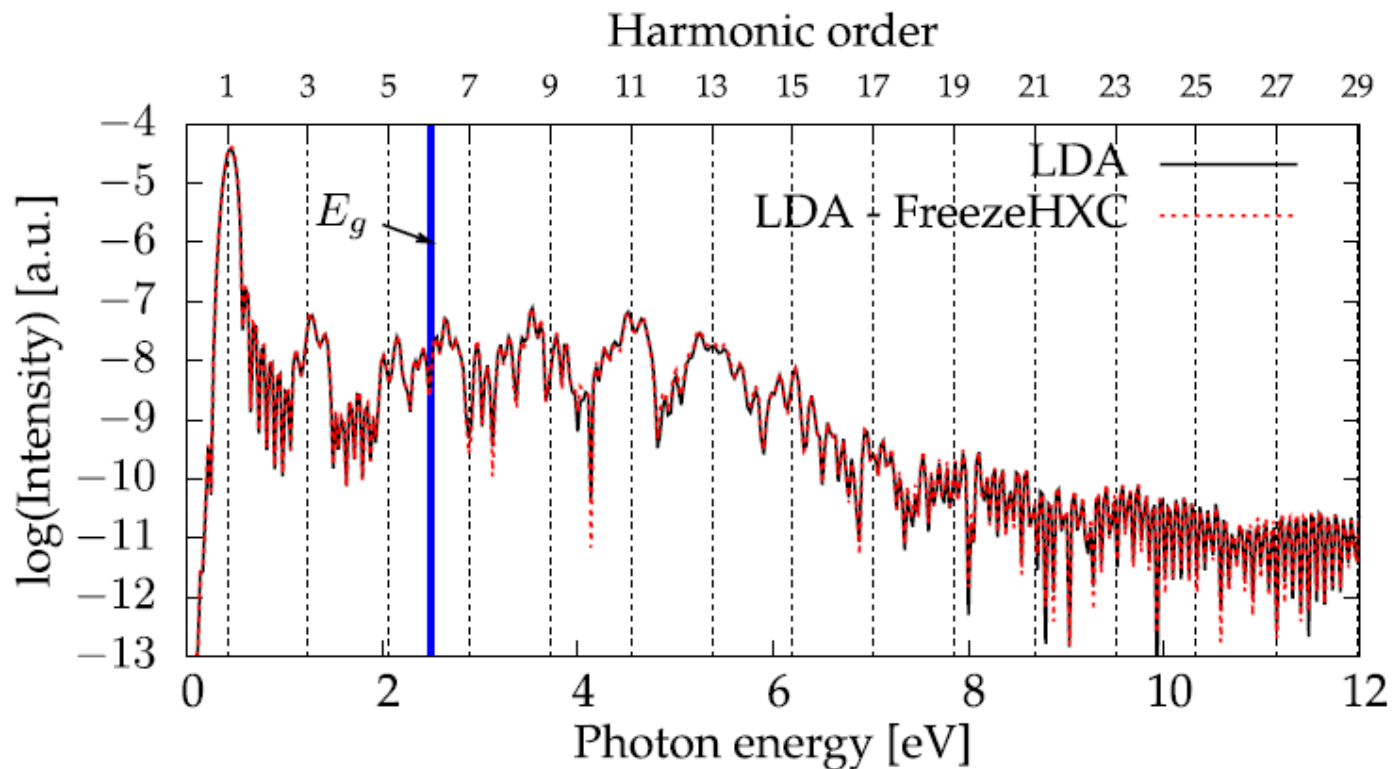


Figure 13.24: HHG spectra from bulk silicon, for polarization along  $\overline{\Gamma X}$ , computed within the LDA (LDA; black line) and within the LDA, but freezing the Coulomb and exchange-correlation terms to their ground-state value (LDA-FreezeHXC; red line). [83]

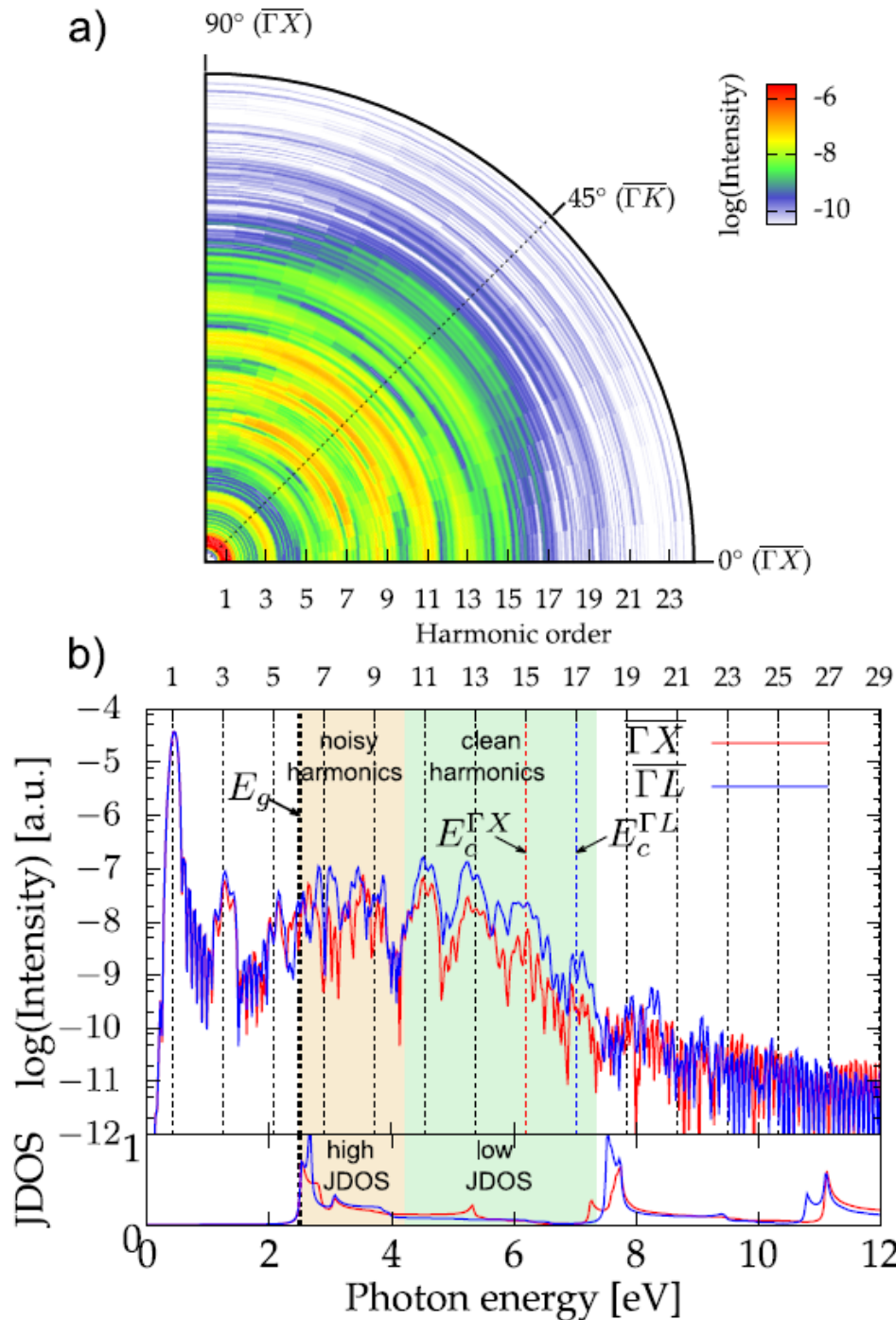
in silicon, electrons evolve mainly as independent particles in the ground-state potential  $\rightarrow$  single-active electron (SAE) approximation good  
 might retrieve ground-state information (band structure) from HHG spectra

**anisotrope HHG emission  
even for cubic crystal**

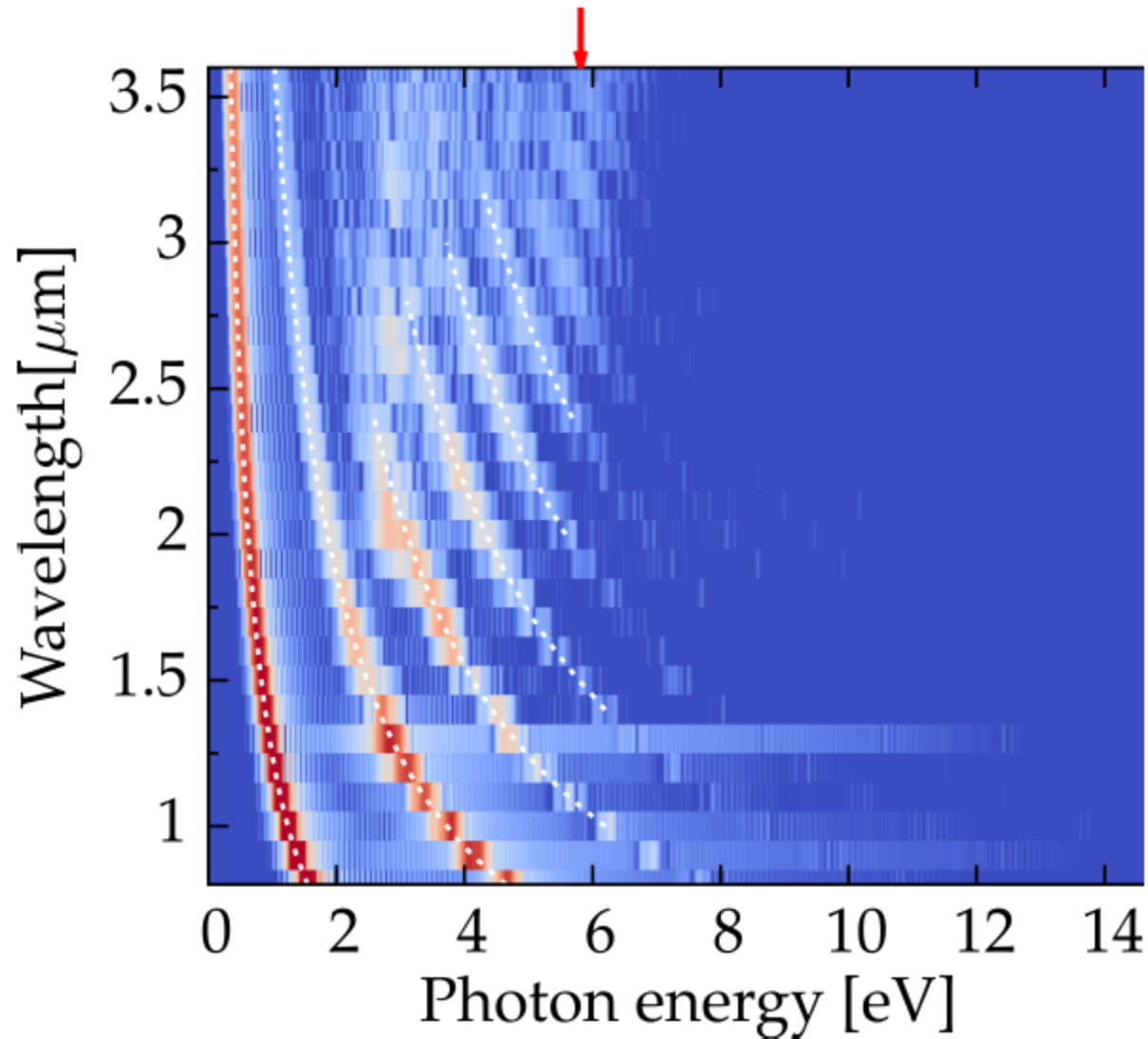
**joint density of state (JDOS)**

low JDOS:  
interband transitions suppressed  
clean harmonics

N. Tancogne-Dejean *et al.*,  
Phys. Rev. Lett **118**, 087403 (2017)



## HHG cutoff independent of driver wavelength



## Summary of findings of

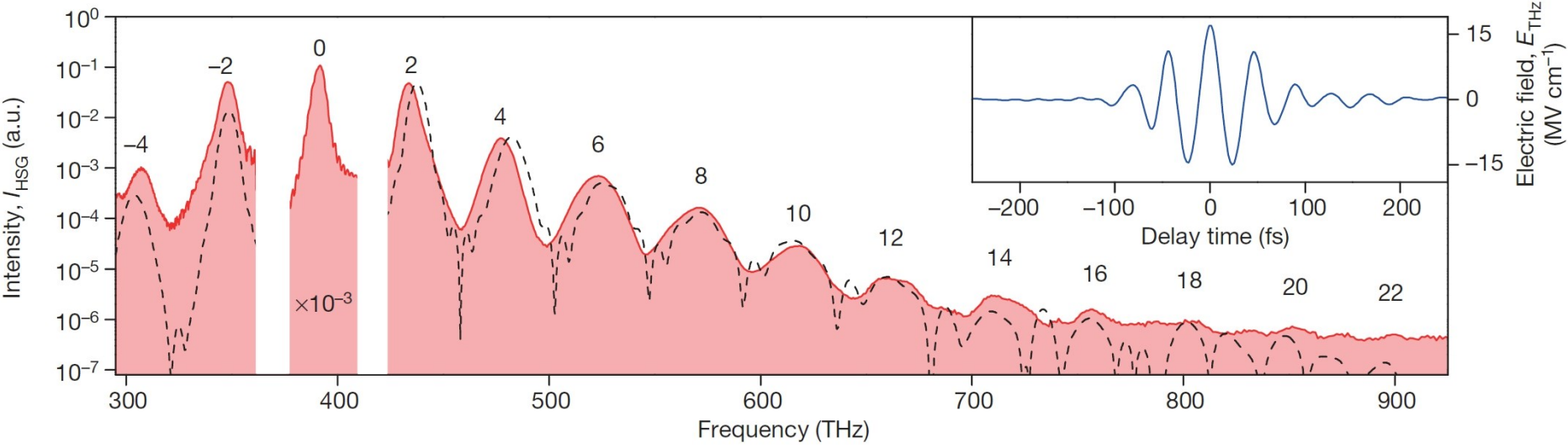
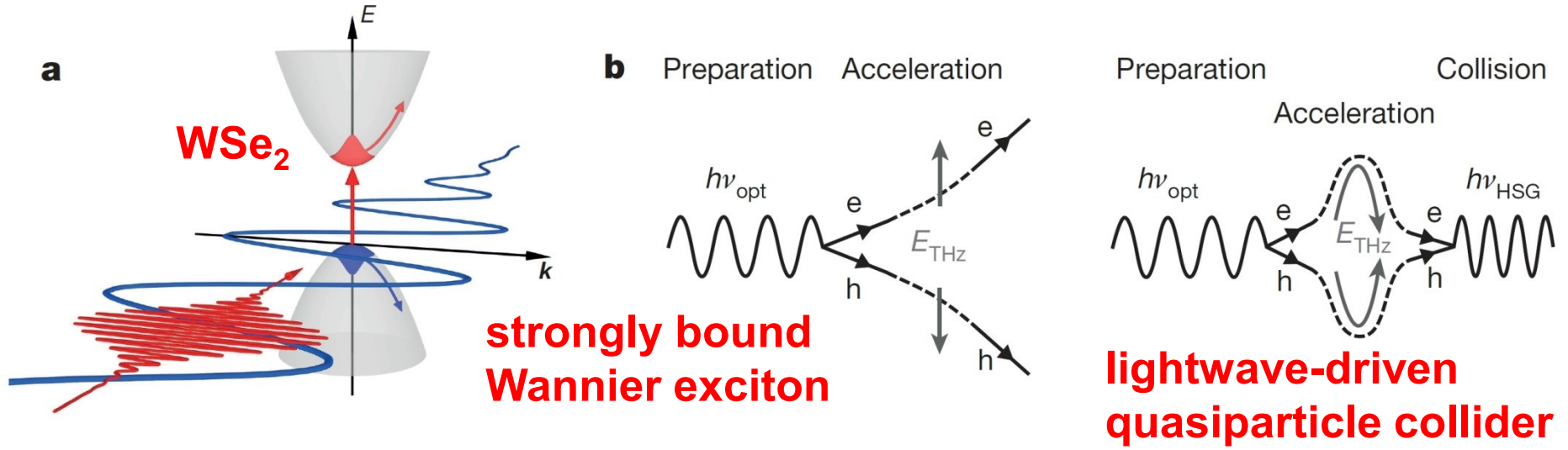
N. Tancogne-Dejean *et al.*, Phys. Rev. Lett **118**, 087403 (2017)

To briefly summarize the findings by Tancogne-Dejean *et al.* [83]: it was shown analytically that HHG in solids is enhanced by the inhomogeneity of the electron-nuclei potential, and that the yield is increased for heavier atoms in the solid. The *ab-initio* TDDFT simulations demonstrated that HHG in bulk crystals is anisotropic, even in cubic materials. The simulations revealed that it is possible to suppress interband transitions in favor of HHG arising from intraband dynamics in solids, and most importantly to predict the optimal laser polarization, based on the sole knowledge of the crystal's band structure and its JDOS. Finally, the simulations confirmed without making any model assumptions that the cutoff of the HHG in solids is wavelength-independent. Further investigations should address extrinsic effects such as the electron-phonon coupling, propagation and surface effects. These findings and *ab-initio* TDDFT simulations can guide the search of better materials for solid-state high-harmonic sources and tailored HHG in solids.

dependence on driver polarization, circularly polarized HHG:

N. Tancogne-Dejean *et al.*, Nature Commun. **8**, 745 (2017)

# 13.7 High-order sideband generation



F. Langer *et al.*, Nature **533**, 225 (2016)

B. Zaks *et al.*, Nature **483**, 580 (2012) THz-FEL

## 13.8 Dynamical Franz-Keldysh effect

### **static Franz-Keldysh effect:**

photon-assisted tunneling of electrons from valence to conduction band

### **dynamical Franz-Keldysh effect:**

characterized by  $U_p \approx \hbar\omega_0$  , can be thought of as the point, where the **tunneling time is comparable to the light period** of the excitation field

## 13.8 Dynamical Franz-Keldysh effect

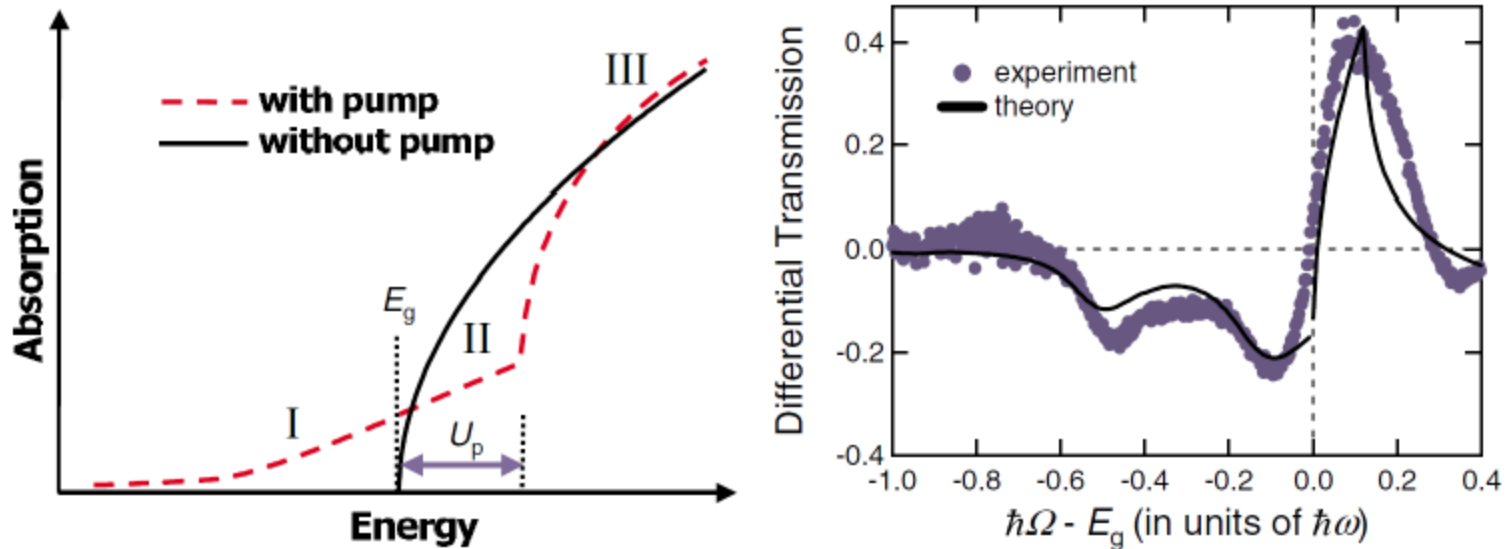


Figure 13.23: Dynamical Franz-Keldysh effect: (Left) Interband absorption in a direct-gap semiconductor near the band gap  $E_g$  without (solid line) and with (dashed line) a strong driving field. (Right) Experimental data in GaAs and fit by Yacoby's [24] theory. [77]

A. Srivastava *et al.*, Phys. Rev. Lett. **93**, 157401 (2004)

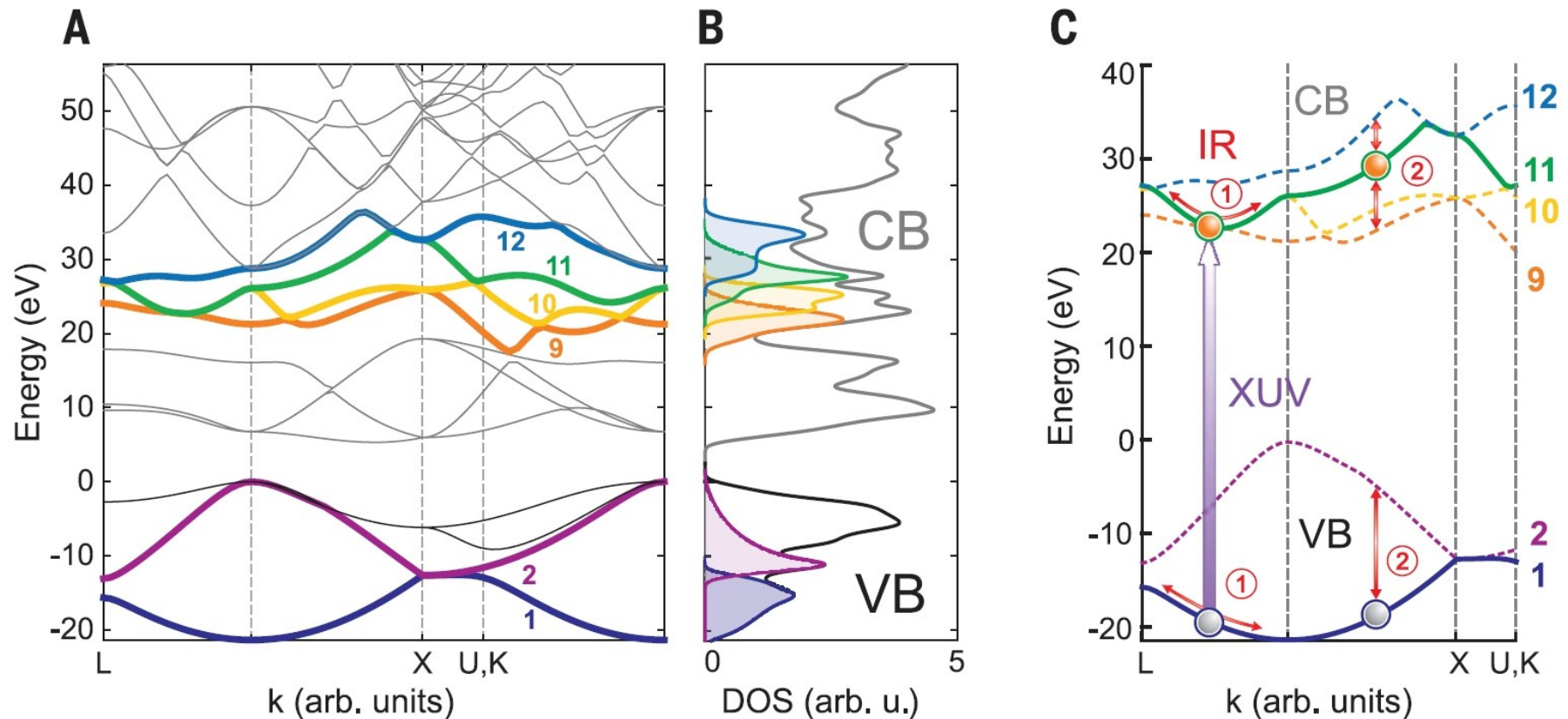
- (i) induced below-band-gap absorption (region I),
- (ii) blue shift (equal to  $U_p$ ) of the band edge causing induced transparency (region II),
- (iii) oscillatory behavior above the band gap (region III)

# attosecond dynamical Franz-Keldysh effect in diamond

attosecond transient XUV absorption on polycrystalline diamond

5-fs IR pump,  $\sim 6.5 \times 10^{12}$  W/cm<sup>2</sup>

isolated 255-as XUV pulses (spectrum 35-50 eV)

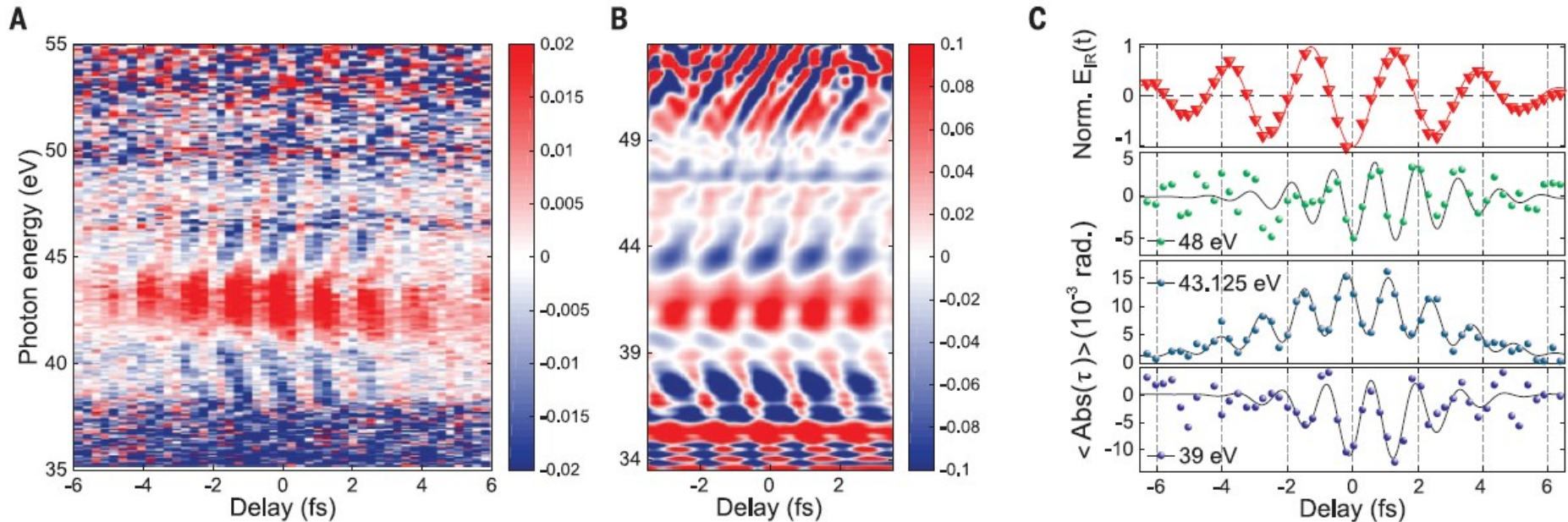


# attosecond dynamical Franz-Keldysh effect in diamond

attosecond transient XUV absorption on polycrystalline diamond

5-fs IR pump,  $\sim 6.5 \times 10^{12}$  W/cm<sup>2</sup>

isolated 255-as XUV pulses (spectrum 35-50 eV)



$$\Delta \text{Abs}(E_{\text{ph}}, \tau) = \Delta \alpha(E_{\text{ph}}, \tau) L = (\alpha_{\text{IR}}(E_{\text{ph}}, \tau) - \alpha_0(E_{\text{ph}})) L = \ln \left( \frac{I_t(E_{\text{ph}})}{I_t^{\text{IR}}(E_{\text{ph}}, \tau)} \right). \quad (13.57)$$

**IR-pump-induced changes oscillate at  $2\omega_{\text{IR}}$**

M. Lucchini *et al.*, Science **353**, 916 (2016)